Abstract for the 30th Intl Workshop on Water Waves and Floating Bodies, April 12-15, 2015, Bristol, UK

Double Doppler shift theory on water waves generated by a translating and oscillating source

Zhi-Ming Yuan, Atilla Incecik, Alexander Day, Laibing Jia

Dep. of Naval Architecture, Ocean & Marine Engineering, University of Strathclyde, Henry Dyer Building, G4 0LZ, Glasgow, UK

Highlights

- Development of double Doppler shift theory
- Application of double Doppler shift theory on the prediction of water waves generated by a translating and oscillating source

Introduction

The V-shaped wakes behind a translating source on calm water have been widely investigated by many researchers, and the wake half-angle $\psi = \arcsin(1/3) \approx 19.47°$. However, as the source point are advancing in waves, the scattered wave patterns become complicated. As indicated by Becker [1] and Noblesse [2], there exists three wave systems (shown in Figure 1 (a)) as the parameter $\tau < 0.25$ ($\tau = \omega_e u/g$, ω_e is the encounter frequency, u is the forward speed, and g is the gravity acceleration): one ring wave system, which are approximately elliptical in shape, and two Kelvin fan wave systems confined within two distinct wedges, which can be referred as 'outer and inner V waves'. At $\tau < 0.25$, as shown in Figure 1 (b), the upstream portion of the ring waves do not exist. The constant-phase curves depicted in Figure 1 can be obtained by the stationary phase method, which is based on the framework of Green function method.

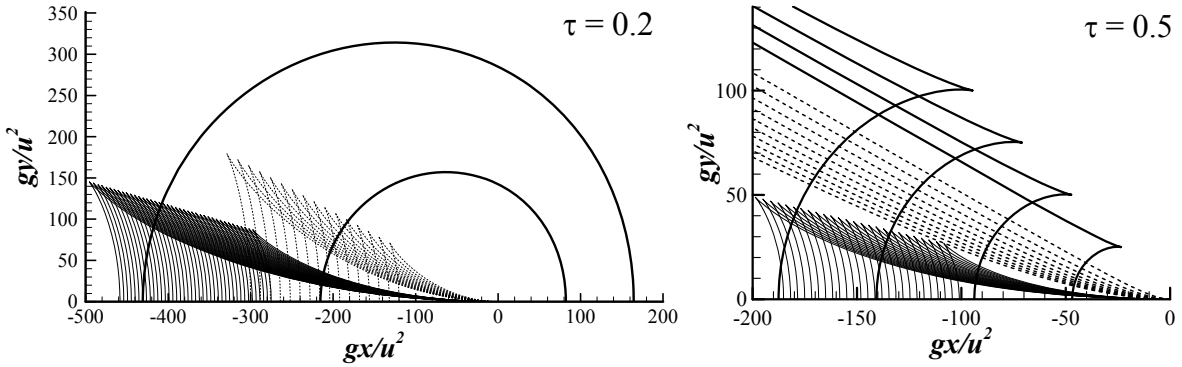

Figure 1 Far-field wave patterns for a translating and pulsating source point located at (0, 0, z), z > 0. (a) $\tau = 0.2$; (b) $\tau = 0.5$.

The present study attempts to establish a method based on physical propagation of the waves to investigate the far-field wave patterns, and this method is referred as double Doppler shift theory hereafter. It should be noticed that the present method was firstly used by Das and Cheung [3] to satisfy the radiation condition for the marine vessels advancing in waves, and Yuan et al. [4] verified this theory through a series of numerical simulation about a single or two ships advancing in waves.

Mathematical expression of double Doppler shift theory

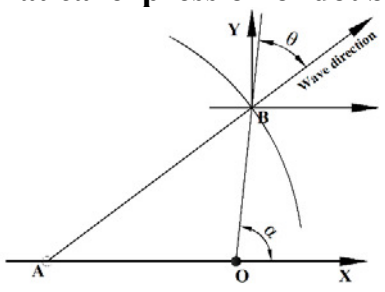

Figure 2 Sketch of the physical propagation of the waves.

Figure 2 shows the propagation of the scattered waves produced by a translating and oscillating source. Supposing there is source point travelling along x-axis from point A to point O with constant forward speed u_0. The traveling time should be $t = AO/u_0$. During this period of time, the translating and oscillating source produces scattered waves all along AO, and the scattered waves produced at point A is propagating to point B. Compared to waves produced at point O, the wave

direction has been rotated by an angle θ. Let's define the velocity of the scattered wave as c, then $AO/u_0 = AB/c$. According to the sine theorem, it can be easily transferred to

$$\frac{u_0}{c} = \frac{\sin\theta}{\sin\alpha} \tag{1}$$

The scattered wave velocity at B can be expressed as

$$c^2 = \frac{g}{k_s}\tanh k_s d \tag{2}$$

where ω_s is the angular frequency of the scattered waves from a fixed reference point given as

$$\omega_s = \omega_e + u_0 k_s \cos(\alpha - \theta) \tag{3}$$

The local dispersion relation for the scattered waves is

$$\omega_s^2 = g k_s \tanh k_s d \tag{4}$$

where k_s is the local wave number at any point on the free surface and d is the water depth. The dimensionless local wave length and local wave number can be defined as

$$\gamma = \frac{2\pi g}{k_s u_0^2}, \quad \kappa = \frac{k_s u_0^2}{g} \tag{5}$$

Combining Eqs. (1)-(5), the following governing equation can be obtained

$$A\kappa^2 + B\kappa + \tau^2 = 0 \tag{6}$$

The coefficient A and B are defined as

$$A = \cos^2\left[\alpha - \sin^{-1}\left(\sqrt{\kappa}\sin\alpha \Big/ \sqrt{\tanh\left(\kappa / F_h^2\right)}\right)\right] \tag{7}$$

$$B = 2\tau\cos\left[\alpha - \sin^{-1}\left(\sqrt{\kappa}\sin\alpha \Big/ \sqrt{\tanh\left(\kappa / F_h^2\right)}\right)\right] - \tanh\left(\kappa / F_h^2\right) \tag{8}$$

where F_h is the depth Froude number and can be written as

$$F_h = \frac{u_0}{\sqrt{gd}} \tag{9}$$

At infinite water depth, $d\to\infty$, Eq. (6) can be reduced to

$$\cos^2\left[\alpha - \sin^{-1}\left(\sqrt{\kappa}\sin\alpha\right)\right]\kappa^2 + \left\{2\tau\cos\left[\alpha - \sin^{-1}\left(\sqrt{\kappa}\sin\alpha\right)\right] - 1\right\}\kappa + \tau^2 = 0 \tag{10}$$

2D wave patterns

Let's firstly discuss the wave length on x-axis. At $\alpha \to 0$ or π, $\sin^{-1}(\kappa\sin\alpha) \to 0$ and Eq. (10) becomes

$$\cos^2(\alpha)\kappa^2 + \left[2\tau\cos(\alpha) - 1\right]\kappa + \tau^2 = 0 \tag{11}$$

The solutions for Eq. (11) can be written as

$$\kappa = \frac{1 - 2\tau\cos\alpha \pm \sqrt{1 - 4\tau\cos\alpha}}{2\cos^2\alpha} \tag{12}$$

In the positive x-axis ($\alpha \to 0$), $\cos\alpha \to 1$ and Eq. (12) can be expressed as

$$\kappa_{1,2} = \frac{1 - 2\tau \pm \sqrt{1 - 4\tau}}{2} \tag{13}$$

Substitute Eq. (13) into Eq.(5), we can obtain the dimensionless local wave length on positive x-axis as

$$\gamma_{1,2} = \frac{4\pi}{1 - 2\tau \mp \sqrt{1 - 4\tau}} \tag{14}$$

In the negative x-axis ($\alpha \to \pi$), $\cos\alpha \to -1$ and Eq. (12) can be expressed as

$$\kappa_{3,4} = \frac{1 + 2\tau \pm \sqrt{1 + 4\tau}}{2} \tag{15}$$

Substitute Eq. (15) into Eq.(5), we can obtain the dimensionless local wave length on negative x-axis as

$$\gamma_{3,4} = \frac{4\pi}{1 + 2\tau \mp \sqrt{1 + 4\tau}} \tag{16}$$

The dimensionless local wave length defined in Eq. (14) and (16) is depicted in Figure 3. The results in Figure 3 are consistent with the solutions provided by Becker[1]. At $\tau < 0.25$, there are four wave systems on the x-axis. At $\tau > 0.25$, the wave systems on positive x-axis vanish and only two wave systems exist on negative x-axis. At $\tau = 0$, the dimensionless local wave length γ_1 and γ_3 (corresponding to the ring wave system, which will be discussed further on) turn to be infinity, and γ_2 and γ_4 merge together as Kelvin wave with the dimensionless local wave length $\gamma = 2\pi$.

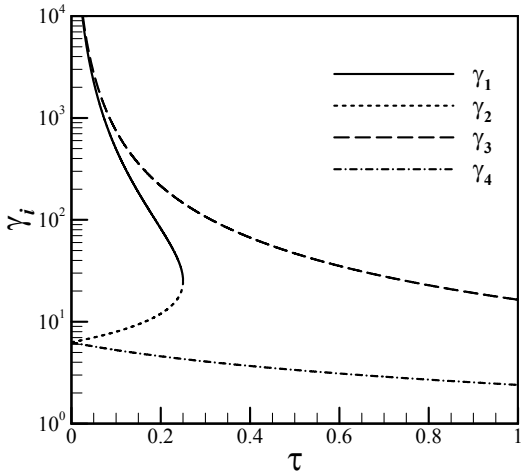

Figure 3 Dimensionless wavelength on x-axis.

It should also be noticed that at infinite water depth, as $\alpha \to \pi$,

$$\omega_s = -\frac{1}{2}\left(1+\sqrt{1+4\tau}\right) < 0 \qquad (17)$$

The physical explanation of this negative local encounter frequency is similar to that of encounter frequency [5]. The apparent direction of the scattered wave propagation is obtained by observation. When $\omega_s < 0$, the ship outraces the waves and their crests actually appear to be moving from the ship's bow toward her stern. Therefore, γ_4 represents the wave length behind the ship propagating in the opposite direction.

3D wave patterns

From Eq. (6) we find the dimensionless local wave number is determined by three independent parameters: τ, F_h and α. For a given τ in infinite water depth, from Eq. (10) it can be found that the dimensionless local wave number is only determined by α. Based on the similar idea of stationary phase method, the curves of equal phase for the various systems of waves can be drawn as α varies from 0 to 2π. For a given α, the nonlinear equation in Eq. (10) can be solved by a numerical iterative scheme. Figure 4 shows the solutions of Eq. (10) for parameter $\tau = 0.25$ and $\tau = 0.5$ at infinite water depth. Typically, there are four solutions for Eq. (10), and these solutions can be only found at some limited range of α. For the case of $\tau = 0.25$, two sets of solution can be found in the entire range of α, and at $\alpha = 0$, these two sets of solution merge at $\kappa = 25.12$. The rest two sets of solution are limited at $\alpha > 162.12°$. For the case of $\tau = 0.5$, two sets of the solution only exist at $\alpha > 107.47°$, and the rest two sets of solution only exist at $\alpha > 163.26°$. As parameter increases, these four solutions become small and are close to each other, and they are limited to a very small range of α, which is approaching 180°.

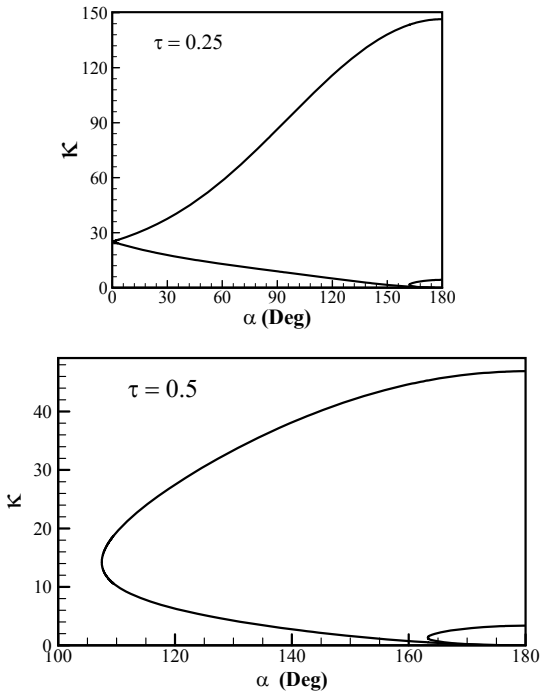

Figure 4 Typical solutions of Eq.(10)

Defining κ_i as the i-th solution for Eq.(10), and each solution corresponds to an independent wave system, then the corresponding points of stationary phase can be written as

$$\begin{cases} x = \dfrac{\psi}{\kappa_i}\cos\alpha \\ y = \dfrac{\psi}{\kappa_i}\sin\alpha \end{cases}, \quad i = 1,2,3,4 \qquad (18)$$

Eq. (18) is parametric equation defining the curves (x, y) along which the phase Ψ remains constant. It can be found from Eq. (18) that the curves are symmetrical about x-axis. Therefore, only the plane of $y \geq 0$ will be displayed hereafter. The constant-phase curves defined by the parametric equation (18) are depicted in Figure 5 for a set of values of Ψ with increment equal to 2π, and for following six values of τ: 0.2, 0.25, 0.26, 0.5, 1 and 4. This figure shows that, for values of τ smaller than 0.25, three distinct wave systems can be identified. These wave systems consist of 'ring waves' which are approximately elliptical in shape, and two wave systems found in two distinct regions. The raindrop-shape wave system appeared downstream can be called 'raindrop waves', and the helical-shape wave system, which appears mainly upstream, can be called 'helical waves'. For value of $\tau = 0.25$, the helical waves merge with the ring waves in the positive x-axis. As $\tau \to 0.25^+$, there is no wave existing in the positive x-axis. For value of $\tau >$ 0.25, the helical waves merge with the ring waves, forming an integrated and closed wave system. And as the parameter τ increases, this integrated wave system shifts downstream, merging with the raindrop-shape wave system gradually.

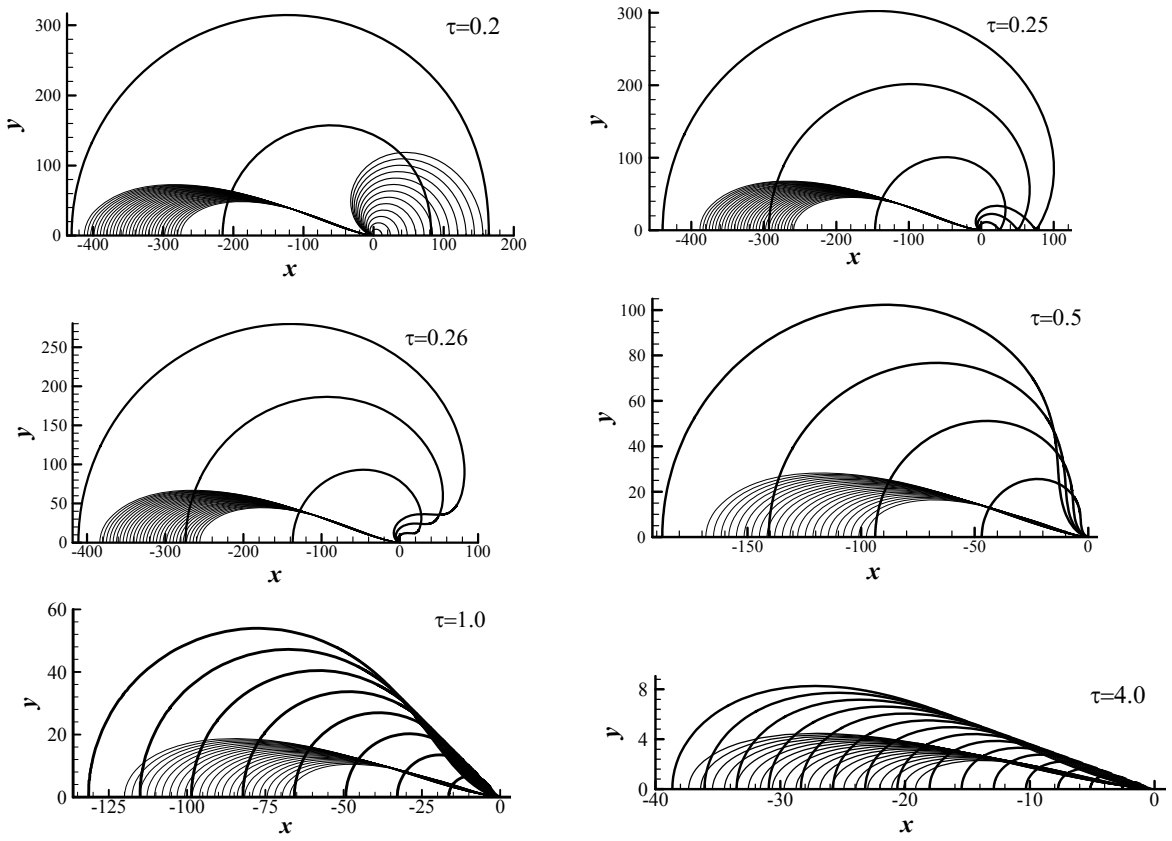

Figure 5 Far-field wave patterns for a translating and pulsating source point with six values of τ: 0.2, 0.25, 0.26, 0.5, 1 and 4.

Steady wave patterns

Particularly, as $\tau \to 0$, Eq. (10) can be reduced to

$$\cos^2\left[\alpha - \sin^{-1}\left(\sqrt{\kappa}\sin\alpha\right)\right]\kappa^2 - \kappa = 0 \tag{19}$$

The solutions for Eq. (19) can be written as

$$\left.\begin{array}{c}\kappa_1 = 1 \\ \kappa_{2,3} = \dfrac{4}{-1+3\cos 2\alpha \pm \sqrt{2\cos^2\alpha(9\cos 2\alpha - 7)}}\end{array}\right\} \tag{20}$$

Substituting Eq. (20) into Eq. (18), we can obtain the constant-phase wave patterns, as shown in Figure 6. κ_1 corresponds to the particular case $u = 0$ and $\omega_e \neq$, and the wave pattern represents the waves generated by a pulsating source. The other case which makes $\tau = 0$ is $u \neq 0$ and $\omega_e = 0$, and the wave pattern represents the waves generated by a translating source. κ_2 and κ_3 are the solutions corresponding to this case. It can be observed from Figure 6 that κ_2 and κ_3 merged into the raindrop waves as $\sqrt{2\cos^2\alpha(9\cos 2\alpha - 7)} \to 0$. The raindrop waves will confined within $\alpha = \frac{1}{2}\cos^{-1}\left(\frac{7}{9}\right) \approx 19.47^\circ$, which is exact the same as Kelvin angle.

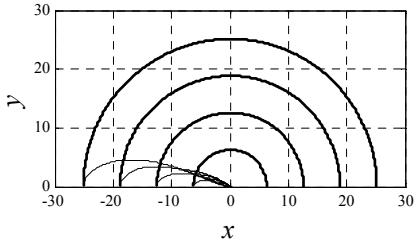

Figure 6 Far-field wave patterns for a translating and pulsating source point at $\tau = 0$.

References

1. Becker, E., *Das Wellenbild einer unter der Oberfläche eines Stromes schwerer Flüssigkeit pulsierenden Quelle.* Journal of Applied Mathematics and Mechanics, 1958. **38**(9-10): p. 391-399.
2. Noblesse, F. and D. Hendrix, *On the theory of potential flow about a ship advancing in waves.* Journal of Ship Research 1992. **36**(1): p. 17-30.
3. Das, S. and K.F. Cheung, *Scattered waves and motions of marine vessels advancing in a seaway.* Wave Motion, 2012. **49**(1): p. 181-197.
4. Yuan, Z.M., A. Incecik, and A. Day, *Verification of a new radiation condition for two ships advancing in waves.* Applied Ocean Research 48, 2014: p. 186-201.
5. Denis, M.S., Member, and W.J. Pierson, *On the motions of ships in confused seas.* Trans. NAME, 1953. **61**.